EOS Microwave Limb Sounder observations of upper stratospheric BrO: Implications for total bromine

Nathaniel J. Livesey,[1] Laurie J. Kovalenko,[1,2] Ross J. Salawitch,[1] Ian A. MacKenzie,[3] Martyn P. Chipperfield,[4] William G. Read,[1] Robert F. Jarnot,[1] and Joe W. Waters[1]

Received 17 May 2006; revised 1 September 2006; accepted 12 September 2006; published 31 October 2006.

[1] This paper describes new total stratospheric inorganic bromine (Br_y) abundance estimates inferred from the first global observations of upper stratospheric BrO, made by the EOS Microwave Limb Sounder on the Aura satellite. Our 'best estimate' of total upper stratospheric bromine loading (based on JPL-2002 kinetics with the addition of a $BrONO_2$ + O reaction) is 18.6 ± 5.5 pptv, for the period September 2004 to August 2005, from 55° S to 55° N. This implies a contribution of 3.0 ± 5.5 pptv from sources other than long lived CH_3Br and halons. The possibility of such other sources has been raised by balloon, aircraft and satellite observations of BrO in the lower and middle stratosphere. These upper stratospheric observations provide new information to help resolve the current uncertainty in stratospheric bromine loading. The abundance of bromine, particularly in the lower stratosphere, is a significant factor in the budget of stratospheric O_3. **Citation:** Livesey, N. J., L. J. Kovalenko, R. J. Salawitch, I. A. MacKenzie, M. P. Chipperfield, W. G. Read, R. F. Jarnot, and J. W. Waters (2006), EOS Microwave Limb Sounder observations of upper stratospheric BrO: Implications for total bromine, *Geophys. Res. Lett.*, *33*, L20817, doi:10.1029/2006GL026930.

1. Introduction

[2] Stratospheric bromine and its role in photochemical O_3 destruction have received much attention in recent studies [e.g., *Salawitch et al.*, 2005]. Estimates of total stratospheric bromine loading based on observations of stratospheric BrO generally indicate 4–6 pptv more bromine than would be expected from contributions of the known long-lived source gases CH_3Br and halons [*World Meteorological Organization* (*WMO*), 2003]. This excess in total inorganic bromine (Br_y) may reflect the contributions of Very Short-Lived (VSL) halogenated species in the stratosphere [e.g., *Wamsley et al.*, 1998; *Pfeilsticker et al.*, 2000] and of upper tropospheric BrO transported into the stratosphere [*Pfeilsticker et al.*, 2000]. Either scenario implies larger abundances of reactive bromine in the lower stratosphere than is often assumed in model simulations of O_3 chemistry. In this region, where the bulk of the chlorine is still in non-reactive organic forms, bromine plays a more significant role in photochemical O_3 destruction than elsewhere, and the rate of O_3 loss is very sensitive to the amount of Br_y [*WMO*, 2003; *Salawitch et al.*, 2005].

[3] In this paper new global observations of upper stratospheric BrO from the Microwave Limb Sounder (MLS) [*Waters et al.*, 2006] on the Aura satellite (launched in July 2004) are used in conjunction with models to infer upper stratospheric Br_y.

2. MLS BrO Observations

[4] MLS observes two sets of BrO emission lines around 640 GHz. Figure 1 shows observations from one of these sets. The 2–3 K noise on individual limb radiance measurements is large compared to the typically 0.1–0.2 K signature of BrO. Significant averaging is required to obtain abundance estimates with a useful signal-to-noise ratio.

[5] Version 1.51 of the MLS data processing algorithms [*Livesey et al.*, 2006], the first MLS data version released for public use, produces ~3500 BrO abundance profiles daily with a typical precision of 200–300 pptv. When averages, such as monthly zonal means, are taken, large amounts of noise are still seen in the data, due to a poor choice of the tradeoff between precision and vertical resolution.

[6] For this study, an 'off-line' BrO algorithm has been developed which produces a pair of zonal mean abundance fields for each day, one for the ascending (mostly daytime) part of the orbit, the other for descending (mostly nighttime). These are retrieved from 10°-latitude-resolution zonal averages of the daily radiance observations. Radiances are binned onto a vertical grid of 12 surfaces per decade change in pressure (~1.5 km), using the limb tangent point pressures from v1.51 data. The daily zonal mean BrO abundances retrieved have an estimated precision of 10–20 pptv in the mid- and upper stratosphere. Seasonal averaging of these gives abundances with a precision of ~2 pptv.

[7] Figure 2 shows seasonal zonal means of the ascending (a) and descending (b) MLS BrO. These show the generally expected behavior, with ~9–15 pptv of BrO seen in much of the upper stratosphere during daytime and essentially zero BrO at night. Lower average BrO abundances are seen on the ascending side of the orbit in polar night regions, while significant abundance is seen on the descending half in the polar day regions.

[8] The descending (mainly nighttime) BrO abundances observed by MLS are unrealistically large around 10 hPa (larger still at greater pressures, not shown). For pressures greater than about 4 hPa, essentially zero BrO is expected at night (2am local time for MLS). The non-zero nighttime abundances therefore indicate systematic biases. (See, how-

[1]Jet Propulsion Laboratory, California Institute of Technology, Pasadena, California, USA.
[2]Columbus Technologies and Services Inc., Pasadena, California, USA.
[3]University of Edinburgh, Edinburgh, UK.
[4]Institute of Atmospheric Science, School of Earth and Environment, University of Leeds, Leeds, UK.

0094-8276/06/2006GL026930

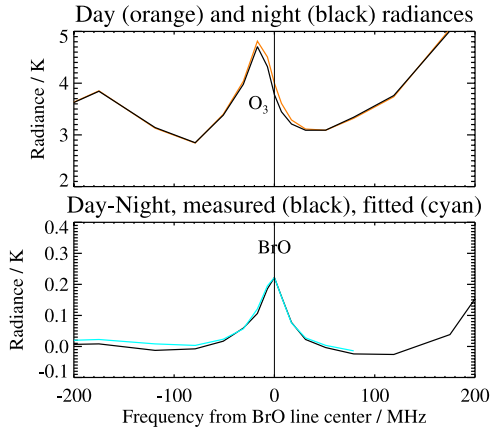

Figure 1. (top) Average upper stratospheric MLS radiances observed in the region of the 650.19 GHz BrO lines. Black line is radiances measured during the descending (nighttime) part of the Aura orbit, orange is ascending (daytime). Average is from 55°S to 55°N, for limb rays with tangent pressures between ~10 hPa and 3.3 hPa, for the period September 2004 to August 2005. The emission signature of an isotopic O_3 line is indicated. (bottom) Difference between day and night measured radiances (black). The BrO spectral signature is clearly seen, due to the strongly diurnal nature of BrO at these altitudes. Cyan line shows the fit achieved to this signal by the retrieval algorithm described in the text.

ever, *Wahner et al.* [1990] for observations of non-zero nighttime lower stratospheric BrO, though those were for winter polar regions, not considered here.) The MLS biases, mainly due to inaccuracies in the retrieval method, become more significant with increasing pressure, as line-broadening increases the contribution of other molecules to the MLS radiances in the BrO spectral region.

[9] Factors that give rise to these biases are expected to be constant between day and night. Accordingly, the difference between day and night BrO observations is a more accurate measure of daytime BrO. Figure 2c shows this difference for the MLS surfaces between 10 and 4.6 hPa. In polar regions, the ascending and descending orbital phases are often both day (summer) or night (winter), so differences in these regions are not useful measures of daytime BrO and are not used in this study (see below for additional discussion of the high-latitude summer data).

[10] This study is confined to data between 55°S and 55°N, with ascending/descending differences used as a measure of daytime BrO for pressures at and larger than the 4.6 hPa MLS pressure surface, and ascending observations alone used for pressures at and smaller than the 3.2 hPa MLS surface. For these latitudes, the local solar time of MLS measurements ranges from 12:50pm to 2:30pm for the ascending part of the orbit, and from 12:50am to 2:30am for descending.

2.1. Accuracy Assessment for the Off-Line BrO Product

[11] Uncertainty in these observations divides into two categories. The first is precision errors due to radiance noise, which can be reduced by averaging. The other category is inaccuracies due to instrument calibration, spectroscopy uncertainty, and retrieval approximations. These terms do not generally average down. However, in our case, neither are they always manifested as temporally constant biases (as discussed below). Instrument calibration and spectroscopic uncertainties are estimated to contribute, respectively, a ±20% and ±3% uncertainty to the MLS BrO.

[12] The accuracy of the retrieval algorithm is estimated by two independent techniques. First, we take advantage of the fact that the off-line algorithms also retrieve O_3 and HNO_3 abundances that are based on observations of ~1–2 K emission lines of these molecules in the vicinity of the BrO lines. One measure of the accuracy of the off-line algorithms is therefore the level of agreement between these products and the well understood O_3 and HNO_3 products produced by the version 1.51 algorithms, which use stronger lines from these species. Second, the accuracy of the linearized forward model used in the retrievals can be quantified by setting all the radiances to zero; the departure of the resulting BrO from the expected zero abundance gives a measure of accuracy.

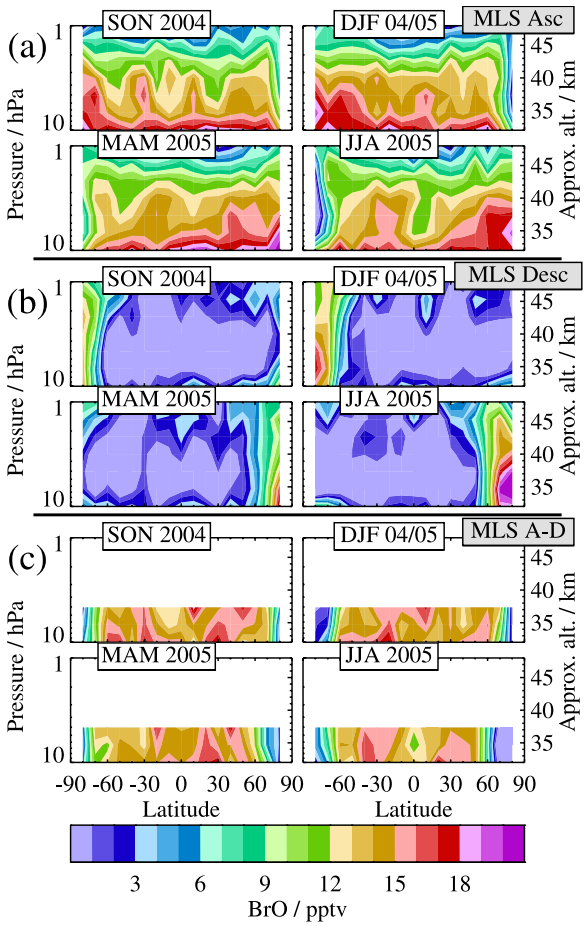

Figure 2. Seasonal zonal means of MLS BrO observations from (a) the ascending (mainly daytime) and (b) descending (mainly nighttime) phases of the orbits. The precision on these averages is 1–2 pptv over the vertical range shown. (c) To alleviate biases in the lower regions, the difference between ascending and descending can be used as a measure of daytime BrO at low and mid-latitudes, so long as the expected nighttime abundance of BrO is negligible, which is the case for MLS data on the 4.6 hPa and greater pressure surfaces.

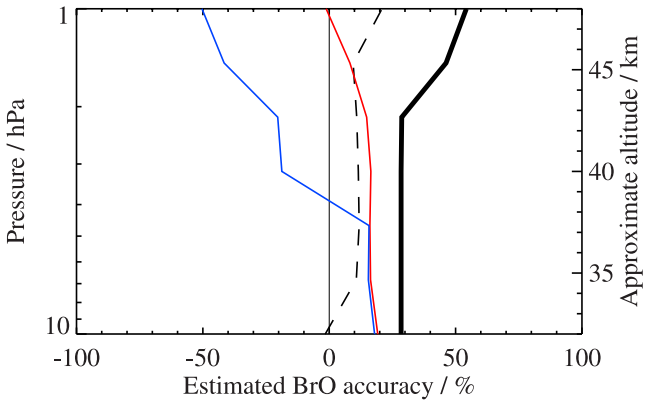

Figure 3. The estimated accuracy of the off-line BrO product. The red and blue lines show the estimates inferred from study of the offline O_3 and HNO_3 products, respectively. The dashed line shows the accuracy predicted from retrievals of zero radiance (scaled from pptv using the annual average 55°S to 55°N profile). The heavy black line shows the overall accuracy estimate, computed as the largest value of the three other lines which is then quadrature summed with the ±3% spectroscopy and ±20% calibration contributions. This results in an estimate of ±30% over the 10–2.2 hPa range.

[13] Figure 3 shows the overall accuracy of the BrO product. This is the quadrature sum of the ±20% calibration, the ±3% spectroscopic uncertainties, and the retrieval accuracy. The latter is summarized as the worst accuracy at each level obtained from the three independent estimates (O_3, HNO_3 and zero radiance). This gives an overall accuracy of ±30% from 10–2.2 hPa. The 1.5 and 1 hPa data are excluded from further consideration due to their poorer accuracy.

[14] Again, note that these accuracy-related uncertainties are not expected to be constant with time/latitude. For example, the accuracy of the retrieval algorithm is driven by departure of the true atmospheric state (O_3, HNO_3, etc.) from that assumed in our linearized forward model. Such errors will exhibit geographic and temporal variability. Figure 2c shows a range of 11–16 pptv BrO for the mid-latitude ascending/descending difference JJA 2005 BrO at ~6.8 hPa, a roughly ±20% scatter about the mean, well within our estimated ±30% uncertainty.

[15] Although we confine our studies to mid-latitudes, we note that Figure 2 shows atypically large values of BrO (~18–20 pptv) around 70° N over 10–4 hPa during JJA 2005 (70° S summer is similar). Day night differences – needed at these altitudes to reduce biases – cannot be taken for these polar day observations. However, studies of these biases show no reason why they should be larger for polar day. This is discussed further below.

[16] Although there have been contemporaneous measurements of BrO obtained by balloon-borne instruments [*Pfeilsticker et al.*, 2000; *Pundt et al.*, 2002], few have had any overlap in altitude range. Future papers will compare these with MLS data.

3. Using Models to Infer Total Bromine

[17] BrO is the dominant form of bromine in the daytime upper stratosphere, accounting for ~60% of the total bromine loading. Two models are used to infer the total stratospheric bromine abundance, needed to assess the impact of bromine on stratospheric O_3.

3.1. SLIMCAT Model

[18] For our analysis, the SLIMCAT model [*Chipperfield*, 1999] is run in 'near-real time' driven by U.K. Met Office analysis fields. Model fields are sampled at the same locations and times (to the nearest 30 minute time step) as the MLS profile observations. By sampling the model in this manner, the diurnal cycle of BrO is fully taken into account. Br_y is inferred according to

$$Br_y^{MLS} = BrO^{MLS}\left(\frac{Br_y^{SLIMCAT}}{BrO^{SLIMCAT}}\right). \quad (1)$$

This run of the SLIMCAT model has been initialized with 16 pptv CH_3Br and 6 pptv of Br_y (representing short lived sources) at the 326 K model boundary. The model shows all of the bromine in Br_y at pressures <30 hPa. Details of the reactions and rates used in both SLIMCAT and our other model are given below. The calculation in (1) is performed for the daily zonal means of SLIMCAT BrO and Br_y, and MLS BrO (ascending and ascending/descending difference, as described above). The resulting daily zonal mean Br_y abundances are further averaged to increase the signal-to-noise ratio.

3.2. Photochemical Diurnal-Steady-State Box Model

[19] In addition to SLIMCAT, a constrained diurnal photochemical steady-state model [*Osterman et al.*, 1997] (PSS hereafter) is used to infer total bromine abundance from the MLS BrO observations. This method was used similarly by *Sioris et al.* [2006]. The PSS model is constrained to MLS observations of temperature, O_3 and water vapor, and also to an NO_y abundance inferred from MLS N_2O observations using well established tracer relations [*Popp et al.*, 2001; *Rinsland et al.*, 1996]. The total bromine loading is treated as a free parameter that is iteratively adjusted until the modeled BrO abundance matches the MLS observations. We ran the model with two sets of kinetics parameters. In one case, which we call JPL02, we used JPL-2002 kinetics [*Sander et al.*, 2003]; in the other, which we call JPL02a, we added the reaction [*Soller et al.*, 2001]

$$BrONO_2 + O \rightarrow BrO + NO_3. \quad (2)$$

While not in the JPL-2002 compendium, this reaction has a large effect on stratospheric bromine partitioning and is also included in SLIMCAT [*Sinnhuber et al.*, 2002].

[20] As with the SLIMCAT calculation, the PSS model is run for the daily zonal mean MLS BrO. The resulting daily Br_y zonal means are averaged to increase the signal-to-noise ratio. As the daily zonal mean MLS BrO is noisy, negative values occur, which cannot be handled by the PSS model. In these cases, the sign is reversed both on the BrO input to PSS (to make it positive) and on the resulting Br_y (back to negative) before averaging.

3.3. Comparison of Br_y Inferred Using Two Models

[21] Figure 4 shows average Br_y profiles obtained using PSS (JPL02 and JPL02a cases) and SLIMCAT. These have

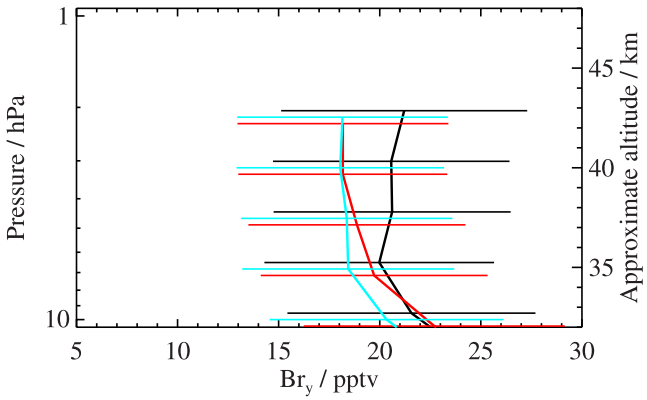

Figure 4. Average Br_y inferred from MLS data using the SLIMCAT (black) and PSS models (red with JPL02 kinetics, cyan with JPL02a). Average is from September 2004 through August 2005, over latitudes from 55°S to 55°N. Error bars reflect the ±30% accuracy of the MLS BrO.

been averaged over one year of MLS measurements, from 55°S to 55°N. The models show good agreement at 10 hPa, but higher in the stratosphere SLIMCAT shows ~2 pptv more Br_y than PSS. This is mainly due to differences in the model abundances of O_3 and NO_y. SLIMCAT computes these, while PSS uses MLS O_3 and NO_y inferred from MLS N_2O. When PSS is run using SLIMCAT O_3 and NO_y and constrained to SLIMCAT BrO, the inferred Br_y matches SLIMCAT's assumed 22 pptv Br_y abundance to within ±0.6 pptv.

[22] Figure 5a compares the vertical profiles of O_3 used in the two models. In the 10 to 2.2 hPa altitude range relevant to our calculation of Br_y, SLIMCAT O_3 is consistently lower than MLS observations (averages over shorter times show the same result). The lower O_3 abundance in SLIMCAT lowers the production rate of BrO via the reactions $HOBr + O \rightarrow BrO + OH$, $BrONO_2 + O \rightarrow BrO + NO_3$, and $Br + O_3 \rightarrow BrO + O_2$ which in turn lowers the BrO/Br_y ratio, increasing the value of Br_y inferred from MLS BrO. In this altitude region, the MLS O_3 measurements have been shown to agree within 10% with other observations [*Froidevaux et al.*, 2006]. The O_3 deficit seen in the SLIMCAT model is well known [e.g., *Osterman et al.*, 1997], although here it is occurring at altitudes lower than expected.

[23] Similarly, there is a systematic difference between the NO_y abundances in the two models, with SLIMCAT consistently showing more NO_y than inferred from MLS measurements of N_2O. Although there are no independent measurements of NO_y, there are sunrise and sunset NO_2 data from the Halogen Occultation Experiment (HALOE) [*Gordley et al.*, 1996] on board the Upper Atmosphere Research Satellite, which measured NO_2 profiles by infrared solar occultation.

[24] Figure 5b compares HALOE sunset data with sunset NO_2 produced by the PSS model, using both tracer-relation-inferred NO_y from MLS N_2O and SLIMCAT NO_y. (Since results at sunset are not output by our SLIMCAT run, we use the PSS model to calculate the diurnal variation of the SLIMCAT model results.) SLIMCAT clearly overestimates the abundance of NO_y in this altitude range. The higher NO_2 in SLIMCAT increases the loss rate of BrO via the reaction $BrO + NO_2 + M \rightarrow BrONO_2 + M$, again increasing the value of Br_y inferred from MLS BrO.

4. Results and Discussions

[25] Further averaging of the results in Figure 4 (i.e., of Br_y averaged from 55°S to 55°N) over the MLS pressure surfaces from 10 hPa to 2.2 hPa gives Br_y estimates of 20.7 pptv from SLIMCAT and 19.2 and 18.6 pptv from PSS for the JPL02 and JPL02a cases, respectively. All three values are estimated to be accurate to ±5.5 pptv. Of the three, the JPL02a case (18.6 pptv) is considered the most accurate as it is based on the most realistic atmospheric abundances of O_3 and NO_y and the most up-to-date reaction rates. The large uncertainty in our results reflects the estimated ±30% accuracy of the MLS BrO product. Future versions of the MLS data processing algorithms should improve this accuracy.

[26] Taken at face value (i.e., without day/night differencing), the high latitude summer BrO abundances discussed earlier imply a Br_y abundance of 24 pptv (PSS JPL02a) and 25 pptv (SLIMCAT). Both of these estimates are just outside the range of our result from lower latitudes. Whether this indicates worse accuracy for these data (for which day/night differencing was not possible) or poorly understood bromine partitioning will be considered in future studies.

[27] From MLS measurements of N_2O in this 10 hPa to 2.2 hPa, 55° S to 55° N region, and the fact that we are considering a 1 year average, we estimate the year of stratospheric entry [*Engel et al.*, 2002] of the air sampled in this study to be 2000 ± 1. Tropospheric CH_3Br and halons are estimated to have contributed 15.6 pptv total bromine at that time [*Montzka et al.*, 2003]. This estimate,

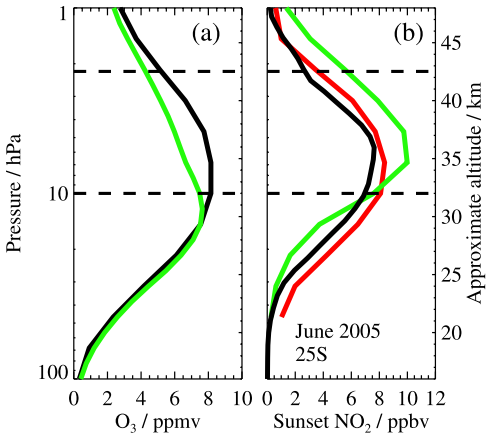

Figure 5. Comparison of vertical profiles of (a) O_3 and (b) NO_2 for the SLIMCAT (green) and PSS (red) models. The dashed lines bracket the relevant altitude region. In Figure 5a the PSS model is constrained to MLS O_3 (black). The profiles are the September 2004 to August 2005 average from 55°S to 55°N. In Figure 5b sunset NO_2 for both models is compared with HALOE data (black). Model daily zonal mean sunset NO_2 are averaged over June 2005 from 15°S to 35°S. The HALOE data (version 19) are averaged over June 2005 from 20°S to 30°S.

based on a global average of tropospheric measurements of these gases obtained over the year 2000, accounts for a 7% loss of CH_3Br in the troposphere, and thus provides a lower limit. A second estimate of 17.0 pptv tropospheric CH_3Br and halons, based on projections from older data [*WMO*, 2003], does not account for any tropospheric loss of CH_3Br, and thus provides an upper limit. From the Montzka estimate, which is based on more recent data, our measurements imply 3.0 ± 5.5 pptv of additional stratospheric bromine from other sources.

[28] This compares well with the estimate of 3 ± 3 pptv obtained from Envisat Scanning Imaging Absorption Spectrometer for Atmospheric Cartography (SCIAMACHY) observations [*Sinnhuber et al.*, 2005], though not so well with another estimate of 8.4 ± 2 pptv, also from SCIAMACHY data [*Sioris et al.*, 2006]. Our observations are at the lower range of the estimates given by *Pfeilsticker et al.* [2000] and *Salawitch et al.* [2005], based on their analyses of aircraft and balloon data. Our results suggest a possible modest contribution of 3.0 ± 5.5 pptv from VSL bromocarbons to the stratospheric bromine budget.

[29] **Acknowledgment.** The research described in this paper was carried out by the Jet Propulsion Laboratory, California Institute of Technology, under a contract with the National Aeronautics and Space Administration.

References

Chipperfield, M. P. (1999), Multiannual simulations with a three-dimensional chemical transport model, *J. Geophys. Res.*, *104*, 1781–1805.

Engel, A., M. Strunk, M. Muller, H. P. Haase, C. Poss, I. Levin, and U. Schmidt (2002), Temporal development of total chlorine in the high-latitude stratosphere based on reference distributions of mean age derived from CO_2 and SF_6, *J. Geophys. Res.*, *107*(D12), 4136, doi:10.1029/2001JD000584.

Froidevaux, L., et al. (2006), Early validation analyses of atmospheric profiles from EOS MLS on the Aura satellite, *IEEE Trans. Geosci. Remote Sens.*, *44*(5), 1106–1121.

Gordley, L. L., et al. (1996), Validation of nitric oxide and nitrogen dioxide measurements made by the Halogen Occultation Experiment for the UARS platform, *J. Geophys. Res.*, *101*, 10,241–10,266.

Livesey, N. J., W. V. Snyder, W. G. Read, and P. A. Wagner (2006), Retrieval algorithms for the EOS Microwave Limb Sounder (MLS), *IEEE Trans. Geosci. Remote Sens.*, *44*(5), 1144–1155.

Montzka, S. A., J. H. Butler, B. D. Hall, D. J. Mondeel, and J. W. Elkins (2003), A decline in tropospheric organic bromine, *Geophys. Res. Lett.*, *30*(15), 1826, doi:10.1029/2003GL017745.

Osterman, G. B., R. J. Salawitch, B. Sen, G. C. Toon, R. A. Stachnik, H. M. Pickett, J. J. Margitan, J. F. Blavier, and D. B. Peterson (1997), Balloon-borne measurements of stratospheric radicals and their precursors: Implications for the production and loss of ozone, *Geophys. Res. Lett.*, *24*(9), 1107–1110.

Pfeilsticker, K., W. T. Sturges, H. Bösch, C. Camy-Peyret, M. P. Chipperfield, A. Engel, R. F. M. Müller, S. Payan, and B. M. Sinnhuber (2000), Lower stratospheric organic and inorganic bromine budget for the Arctic winter 1998/99, *Geophys. Res. Lett.*, *27*(20), 3305–3308.

Popp, P. J., et al. (2001), Severe and extensive denitrification in the 1999–2000 Arctic winter stratosphere, *Geophys. Res. Lett.*, *28*(15), 2875–2878.

Pundt, I., J. P. Pommereau, M. P. Chipperfield, M. V. Roozendael, and F. Goutail (2002), Climatology of the stratospheric BrO vertical distribution by balloon-borne UV–visible spectrometry, *J. Geophys. Res.*, *107*(D4), 4806, doi:10.1029/2002JD002230.

Rinsland, C. P., et al. (1996), ATMOS meaurements of $H_2O + 2CH_4$ and total reactive nitrogen in the November 1994 Antarctic stratosphere: Dehydration and denitrification in the vortex, *Geophys. Res. Lett.*, *23*(17), 2397.

Salawitch, R. J., D. K. Weisenstein, L. J. Kovalenko, C. E. Sioris, P. O. Wennberg, K. Chance, M. K. W. Ko, and C. A. McLinden (2005), Sensitivity of ozone to bromine in the lower stratosphere, *Geophys. Res. Lett.*, *32*, L05811, doi:10.1029/2004GL021504.

Sander, S. P., et al. (2003), Chemical kinetics and photochemical data for use in atmospheric studies, evaluation number 14, technical report, Jet Propul. Lab., Pasadena, Calif.

Sinnhuber, B. M., et al. (2002), Comparison of measurements and model calculations of stratospheric bromine monoxide, *J. Geophys. Res.*, *107*(D19), 4398, doi:10.1029/2001JD000940.

Sinnhuber, B. M., et al. (2005), Global observations of stratospheric bromine monoxide from SCIAMACHY, *Geophys. Res. Lett.*, *23*, L20810, doi:10.1029/2005GL023839.

Sioris, C. E., et al. (2006), Latitudinal and vertical distribution of bromine monoxide in the lower stratosphere from Scanning Imaging Absorption Spectrometer for Atmospheric Chartography limb scattering measurements, *J. Geophys. Res.*, *111*, D14301, doi:10.1029/2005JD006479.

Soller, R., J. M. Nicovich, and P. H. Wine (2001), Temperature-dependent rate coefficients for the reactions of $Br(^2P_{3/2})$, Cl $(^2P_{3/2})$ and $O(^3P_J)$ with $BrONO_2$, *J. Phys. Chem. A*, *105*, 1416–1422.

Wahner, A., J. Callies, H. P. Dorn, U. Platt, and C. Schiller (1990), Near UV atmospheric absorption-measurements of column abundances during Airborne Arctic Stratospheric Expedition, January–February 1989 3: BrO observations, *Geophys. Res. Lett.*, *17*(4), 517–520.

Wamsley, P. R., et al. (1998), Distribution of halon-1211 in the upper troposphere and lower stratosphere and the 1994 total bromine budget, *J. Geophys. Res.*, *103*(D1), 1513–1526.

Waters, J. W., et al. (2006), The Earth Observing System Microwave Limb Sounder (EOS MLS) on the Aura satellite, *IEEE Trans. Geosci. Remote Sens.*, *44*(5), 1075–1092.

World Meteorological Organization (2003), Scientifc assessment of ozone depletion, technical report, Geneva, Switzerland.

R. F. Jarnot, L. J. Kovalenko, N. J. Livesey, W. G. Read, R. J. Salawitch, and J. W. Waters, Jet Propulsion Laboratory, California Institute of Technology, Pasadena, CA 91109, USA. (livesey@mls.jpl.nasa.gov)

I. A. MacKenzie, University of Edinburgh, Edinburgh EH8 9YL, UK.

M. P. Chipperfield, Institute of Atmospheric Science, School of Earth and Environment, University of Leeds, Leeds LS2 9JT, UK.